44th AIAA Aerospace Sciences Meeting and Exhibit
9 - 12 January 2006, Reno, Nevada

AIAA 2006-1384

Design of a MHz Repetition Rate Pulse Burst Laser System at Auburn University

Brian S. Thurow* and Aman Satija†
Auburn University, Auburn, AL, 36849

A next generation pulse burst laser system with repetition rate exceeding 5 MHz is described. The pulse burst laser at Auburn University is based on earlier generation systems, but includes two distinct changes to the basic design. The 1st change is that the pulse slicing is achieved using an acousto-optic modulator (AOM) rather than a pair of electro-optic Pockels cells. The AOM is less expensive (by ~90%) and is able to produce flexible bursts of pulses with variable pulse durations (as short as 10 nsec) at repetition rates ranging from DC to greater than 5 MHz. The energy of the pulses prior to amplification is estimated to be from 0.5 to 3.3 nJ for 10 to 50 nsec long pulses, respectively. The contrast ratio of the pulses produced by the AOM is ~800:1 before spatial filtering and ~15,000:1 after spatial filtering. The 2nd major change in the design of the laser system is the temporal shape of the gain curve created by the power amplifier chain. The design of the flashlamp controller has been specified to produce approximately uniform gain over a 1 msec long period of time. This is contrast to previous designs, which had 100-200 µsec long gain curves with Gaussian shaped profiles. Preliminary measurements show that the total gain for the amplifier chain is approximately 10^7 resulting in individual pulse energies on the order of 10 mJ/pulse. This level of gain is expected to drop by only 10% over the 1 msec duration of gain envelope.

I. Introduction

The use of lasers in flow diagnostics has increased substantially over the last few decades as laser and camera technologies have advanced. Laser based techniques, such as particle image velocimetry, laser Doppler velocimetry and planar laser induced fluorescence are now well developed and prevalent in research laboratories around the world. A common shortcoming to these techniques, however, is the maximum repetition rate they can achieve (10s of Hz). The primary technological limitation is the laser system, which must be able to produce short duration pulses with pulse energies between 1 – 300 mJ/pulse for typical laboratory experiments. Pulsed Nd:YAG lasers, which are solid-state and relatively easy to operate and maintain, are most commonly used to meet these requirements. The overall efficiency of these systems, however, is limited by the broadband output of the flashlamps used for pumping, resulting in a large amount of thermal loading on the system. The thermal loading subsequently limits the pulse repetition rates of Nd:YAG based laser systems to the order of 10 – 100 Hz. One way of circumventing this issue is the pulse burst concept, which allows the system to operate at high repetition rates over a short period of time while keeping the overall duty cycle (average power) low. In this fashion, the thermal load on the system is kept within manageable limits.

This paper describes the design of a new pulse burst laser system at Auburn University. The design is based on laser systems previously developed at Princeton University[1,2,3] and The Ohio State University.[4,5] Similar systems have also been built recently for NASA[6] and the University of Illinois.[7] The basic scheme employed in these systems has been that of a master oscillator power amplifier (MOPA), where a burst of pulses is formed initially at low power and subsequently amplified through a chain of flashlamp pumped power amplifiers. The master oscillator consists of a low power (20 – 100 mW) continuous wave (cw) Nd:YAG laser operating at 1.064 microns. The cw laser beam is then preamplified and double-passed through a pair of Pockels cells, which are used to slice the cw laser beam into a burst of low energy pulses. Following formation of the low energy burst of pulses, the pulses are passed through a series of flashlamp pumped Nd:YAG rod power amplifiers with an overall system gain of 10^6 to 10^8, resulting in pulse energies ranging from 1 – 100 mJ/pulse. The utility of the pulse burst laser system

* Assistant Professor, Dept. of Aerospace Eng., thurow@auburn.edu, AIAA Member.
† Graduate Research Assistant, AIAA Student Member.

for fluid dynamic measurements is well demonstrated and the motivation for the development of the current system.[1-9] The design of the laser system described in this paper includes two distinct changes to the basic design that give it unique capabilities when compared to these other systems.

The first change is to the pulse slicing mechanism, which in the earlier generation systems is conducted using a pair of Pockels cells. Commonly used for Q-switching, Pockels cells are electro-optic devices that cause a polarization retardation to a laser beam when a high voltage (several kV) is applied. For the formation of short duration pulses, the high voltage signal to the electro-optic crystal must be cycled on and off very rapidly. While the rise time can be kept to the order of 3-5 nsec, the fall time on the pulse is much greater. This necessitates the use of a 2nd Pockels cell to form a fast falling edge for the pulse, thus allowing pulse durations of 10 nsec. This process can be repeated quite rapidly, thus allowing for a burst of pulses to be formed with inter-pulse timing as short as 1 μsec (1 MHz). The main problem with this approach is that a pair of Pockels cells and associated high-speed/high-voltage electronics are quite expensive (order $60k). In this paper, the use of a more economical (<$6k) acousto-optic modulator for pulse slicing is described.

The 2nd change involves the length and shape of the gain curve associated with the Nd:YAG rod power amplifier chain. In earlier systems, the gain of the amplifier system varies with time (i.e. gain curve) appearing as a Gaussian shaped profile in time with a width of 100 – 200 μsec. The gain is then superimposed on the burst of pulses resulting in a non-uniform distribution of energy over the pulses, particularly for long bursts of pulses. The problem is exasperated further during the latter stages of amplification, where the gain stored in the rods is depleted by the passage of each pulse. This limits the applications for the laser as pulses are confined to a 100 – 200 μsec window. For the system described in this paper, the gain curve has been modified to have a more uniform 'top hat' profile with an effective length of greater than 1 msec.

II. Overview

The design of the AU pulse burst laser system can be divided into two fundamental parts: 1) the pulse slicer; and 2) the power amplifier chain. The function of the pulse slicer is to slice the output of a cw laser into a burst of low energy (order nJ) pulses. The power amplifier chain is subsequently used to amplify the laser pulses by a factor of $\sim 10^7$. The overall design of the AU pulse burst laser system is similar to previously described systems at Princeton University[1-3] and The Ohio State University,[4-5] but includes some significant changes to improve the affordability and performance of the system. Section III describes the use of an acousto-optic modulator (AOM) for pulse slicing. Section IV describes the design of the amplifier chain where the shape and duration of the gain curve has been modified to be more uniform and longer. Lastly, Section V discusses future improvements planned for the system, such as a more complete characterization of the pulse bursts, the installation of more amplifiers and the addition of a harmonic generator.

III. AOM Pulse Slicer

A burst of low energy laser pulses can be formed by slicing the output of a continuous wave (cw) laser beam. In previous designs, this slicing was achieved using a pair of Pockels cells, which can form pulses less than 10 nsec in duration and at repetition rates as high as 1 MHz. Although effective, this method of slicing is not used here for multiple reasons. First, a pair of high-speed Pockels cells and associated high-speed/high-voltage electronics is not readily available as an 'off-the-shelf' system and must be specially designed and built for the current application. As such, and perhaps most importantly, they are quite expensive (order of $60k). In addition, the high voltage electronics present some safety and reliability concerns and would not be easily replaceable in the event of failure. Lastly, the original manufacturer of the pulse slicers used in the previously discussed systems is out of business and there would be some additional risk associated with trying a new design. An alternative, and much more economical (~$6k), method of creating a burst of pulses from a cw laser beam is through the use of an acousto-optic modulator (AOM).

A. AOM Concept

AOMs, also commonly referred to as Bragg cells, operate on the principles of the acousto-optic effect, where an acoustic wave traveling through a crystal or liquid causes a small variation in the index-of-refraction. This variation appears to an optical beam passing through the medium as a sinusoidal grating with wavelength equal to the acoustic wavelength. Thus, incident light will be diffracted in the presence of the acoustic wave. Most AO devices operate in the Bragg regime, where most of the incident light can be diffracted into the 1st order with the remaining modes

(not including the 0th) annihilated by destructive interferences. This form of diffraction occurs at the Bragg angle, θ_B, given by:

$$\theta_B = \frac{\lambda F_a}{2V_a} \tag{1}$$

where λ is the wavelength of light in air, F_a is the acoustic frequency and V_a is the acoustic velocity. By modulating the intensity of acoustic waves, via a piezoelectric transducer bonded to the crystal, the amplitude of the deflected light can be controlled. Other applications include beam deflection and frequency shifting, where the acoustic frequency is varied as opposed to the intensity.

For the current application, we are interested in slicing pulses of light from a cw laser beam. This can be done by rapidly turning the deflection 'on' or 'off' via control of the acoustic waves inside the AO crystal. In this case, the deflected laser beam constitutes the desired burst of pulses with the beam only being deflected when a positive voltage is applied to the AOM driver. As we are interested in the formation of short duration (10s of nsec) pulses, the most important properties are the rise/fall time, diffraction efficiency and contrast ratio of the AOM and driver.

The rise time, t_r, of the deflected pulse is primarily limited by the time it takes for the acoustic wave to travel across the aperture of the beam and is given by:

$$t_r = \frac{D}{V_a} \tag{2}$$

where D is the diameter of the focused beam within the AO medium. With acoustic velocities on the order of several thousand meters per second, rise times of a few nanoseconds can be achieved by tightly focusing the beam inside the crystal. Additional factors that can affect the rise time of the laser pulses are the intensity profile of the incident beam (e.g. TEM_{00}) and the speed of the AOM RF driver and pulse generator. In this work, a rise time of ~10-15 nsec has been achieved, which is slower than the 3-4 nsec rise times achieved with Pockels cells, but still fast enough for the intended applications of the laser.

The diffraction efficiency of an AOM is a measure of how much of the incident laser energy can be directed into the 1st diffraction mode. It depends on the acoustic power, material properties, geometry and wavelength of light. In general, the intensity of the diffracted beam can range from a few percent to >90 % of the incident beam. An overall efficiency of ~50% after spatial filtering is realized in the current work, which is about half of the >90% efficiency achieved with Pockels cells. Unlike some other AOM applications, such as q-switches, the pulse slicer is not an intra-cavity device. Thus, the poor efficiency of the AOM does not result in an exponential decrease in power as it would if it were placed within an oscillator. Rather, the reduction can be compensated for by increasing the duration of the pulse or building more gain into the amplifier system. It is important to keep in mind that due to saturation, doubling the pulse energy at this early stage does not necessarily correspond to a doubling of pulse energy after amplification.

Lastly, the contrast ratio of the AOM is another important parameter and is given as:

$$CR = \frac{I_{on}}{I_{off}} \tag{3}$$

where I_{on} is the intensity of light when the AOM is turned 'on' and I_{off} is the intensity of laser light with the AOM turned nominally 'off'. The contrast ratio is important because any light passing through the amplifiers when the slicer is off (i.e. when no pulses are desired) will be amplified and reduce the overall efficiency of the system. Because the slicer is off much longer than it is on (by ~3 orders of magnitude), this can cause a significant loss of the energy stored in the amplifiers and limit the energy available for gain to the pulses. The intensity of light when the AOM is turned off is primarily caused by impurities in the crystal, scattered/diffracted light from various optics in the system and leakage RF power from the modulator driver. Typical AOMs have CR ranging from 500 to 1000, which is similar to that achieved using Pockels cells. The CR can be increased by spatially filtering the diffracted laser beam, which helps minimize the contribution of scattered/diffracted light, and using a modulator driver with high extinction ratio.

B. AOM Pulse Slicer Design

Figure 1 is a schematic of the AOM pulse slicer and Figure 2 is a photograph of the system. The overall footprint of the pulse slicer arrangement are ~60 x 30 cm. The master oscillator is a 100 mW single longitudinal mode Nd:YAG cw laser (CrystaLaser, Reno, NV) with output at 1.064 microns. The 0.4 mm diameter beam of the cw laser is first expanded using a -15 mm focal length plano-concave lens and then focused into the AOM with a 50

mm f.l. plano-convex lens to produce a spot size of approximately 40 microns. The AOM (Brimrose GPM-400-100-1060) is mounted on a stage that provides both rotation and translation so that the focused spot can be positioned within the active portion of the AO crystal with an incident angle equal to the Bragg angle. The AO crystal is Gallium Phosphide, which has an acoustic velocity of 6300 m/s. This gives a calculated minimum rise time of ~6 nsec according to Eq 2. The acoustic wave within the crystal is powered by a 1.5 W, 400 MHz RF Source (Brimrose FFA-400-B2-F1.5-X). It has a specified rise time of 3.5 nsec and an extinction ratio >50 dB. The modulation is controlled via an externally applied TTL signal (Quantum Composers 9514+, ~3nsec rise time) and has a digital modulation bandwidth of DC-100 MHz. Thus, bursts with repetition rates as high as 100 MHz are possible. The AOM is able to direct approximately 60% of the incident power into the 1st order with the 0th order blocked by a beam block (to be replaced by a circular aperture). The resulting burst of pulses ($\Delta\theta$= 67mrad) is collimated and directed through a spatial filter with a 50 micron pinhole to improve contrast ratio and mirrors are used to direct the output to the amplifier system.

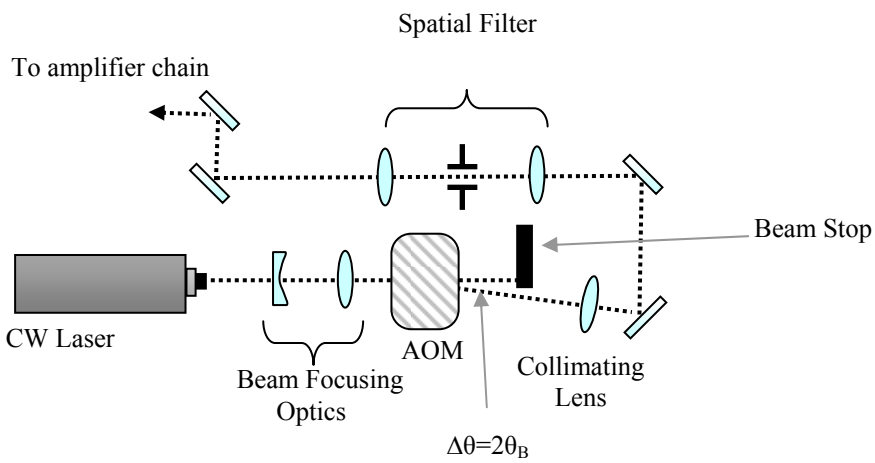

Figure 1 – Schematic of pulse slicer using acousto-optic modulator.

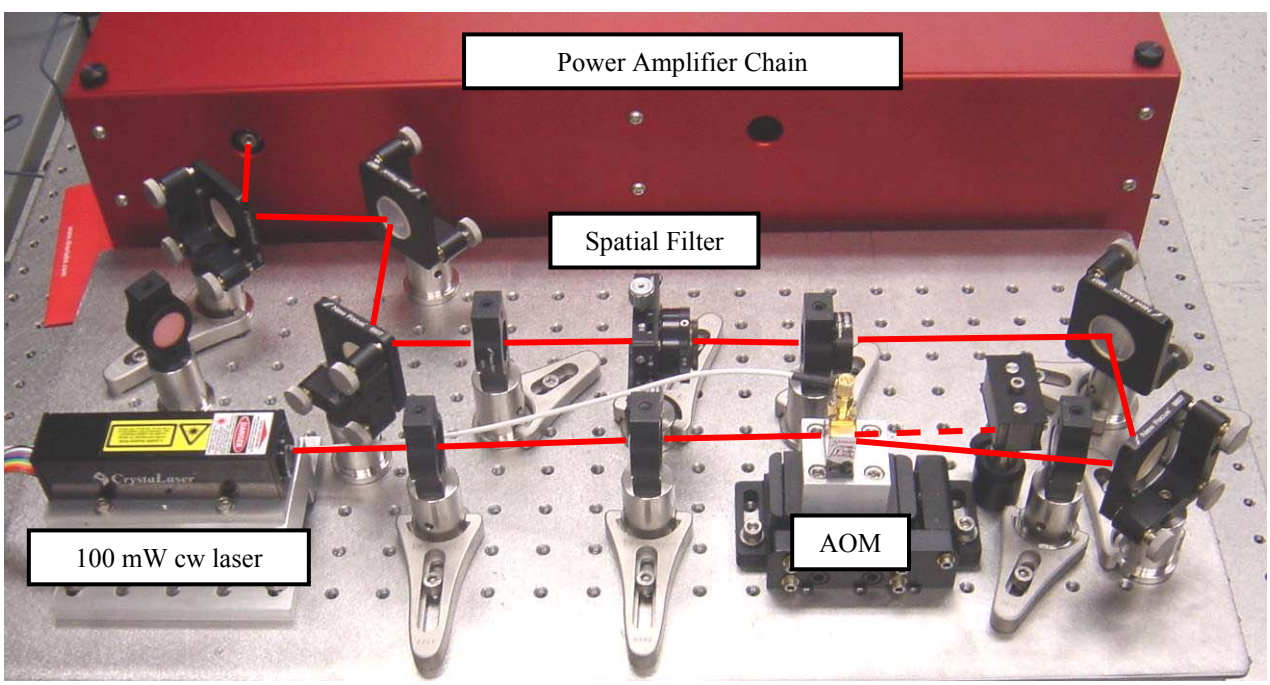

Figure 2 – Photograph of AOM pulse slicer arrangement.

C. Pulse Characteristics

Figure 3 shows oscilloscope traces (500 MHz, Tektronix TDS5054B) for pulses ranging from 10 to 50 nsec in duration (FWHM). The waveforms were acquired with a high-speed photo detector (Thorlabs DET210) with a rise time of 1 nsec. The photo detector was placed after the spatial filter and the waveforms represent the general nature of the pulses that will be seen by the power amplifier chain. The peak power is estimated to be 50 mW, which is the power measured when the beam is continuously deflected by the AOM. For the short duration pulses shown in Figure 3, the power rapidly rises during the 1st 10-15 nsec of the pulse formation. After that, the power continues to slowly rise until it levels out. It is not clear if this slow increase in power between 15 and 35 nsec is optical in nature or an artifact of the measurement technique.

The use of an AOM to produce laser pulses adds some complexity to the measurement as one must account for the acoustic wave traveling across the aperture of the beam. This will cause the power to vary in both space and time, thus making the position of the detector within the beam path important. To capture the entire spatial extent of the pulse, the beam must be focused onto the active area of the detector. Under these conditions, it was found that the linearity limit of the detector was exceeded, making accurate amplitude measurements difficult with the current set-up. Regardless of these issues, the measurements shown in Figure 3 still reveal the most important features of the pulses, namely, the duration and approximate shape of the pulse.

The measured rise/fall time of the pulses is approximately 10 - 15 nsec, not accounting for the slow signal increase between 15 and 35 nsec. This agrees relatively well with an expected rise time of ~8 nsec when the rise time of the pulse generator (3 nsec), modulator driver (3.5 nsec) and acoustic velocity (~6 nsec, Eq. 2) are taken into account.

The approximate energy in each pulse was determined by measuring the average power when the pulses are produced at a 10 kHz repetition rate. The average power measurement (J/sec) is then divided by 10,000 (pulses/sec) to get the energy in each pulse. Pulse energies are estimated to be ~0.5, 1.1, 1.7, 2.6 and 3.3 nJ for 10, 20, 30, 40 and 50 nsec pulses, respectively. Integrating the pulse shapes shown in Figure 3 and assuming a peak power of 50 mW yields similar results.

The contrast ratio of the pulses was determined by measuring the power with the AOM turned off and the cw laser turned on. A Coherent LM-2 VIS power detector with sensitivity as low as 10 nW was used to detect the small amount of laser light that leaks through when the AOM is off. Without a spatial filter in place, approximately 60-90 μW of laser light was detected even with the AOM turned off. 60 mW was measured with the AOM on. This yields a contrast ratio of ~800 +/- 200. This is similar in magnitude to what would be expected with a pair of Pockels cell.

Spatially filtering the signal helps minimize the contribution of background light that is due to off axis scattering caused by impurities in the crystal, diffraction from lenses and other optics, or even dust in the air. With spatial filtering, the background signal is reduced to approximately 3 – 3.5 μW. The drawback to spatial filtering is that it reduces the signal slightly, which was measured to be 50 mW with the AOM on. These measurements result in a contrast ratio of ~15,000 +/- 2000.

After spatial filtering, the contrast ratio is significantly higher than would be expected using a pair of Pockels cells for slicing. One reason for this is that pulses produced deflected by the AOM follow a different optical path than the incident cw laser beam, thus making it easier to separate the pulses from the cw beam. The contrast ratio can be further increased by the addition of a 2nd AOM which could serve as a gate for the pulse slicing AOM. Alternatively, after further amplification of the pulses, a phase conjugate mirror could be used as described by Thurow et al.[4]

The formation of pulses by the AOM can be repeated at repetition rates up to 100 MHz. The high repetition rate capabilities of the current system are demonstrated in Figure 4, which displays a burst of four 20 nsec long pulses separated in time by 200 nsec each (5 MHz). In this case, the repetition rate is limited by the pulse generator and not the AOM. Higher repetition rates should be possible with more advanced pulse generators. For fluid dynamic measurements, a more applicable burst of pulses shown in Figure 5. The figure shows a bursts of 100 pulses with 20 nsec duration separated by 10 microseconds each (100 kHz). This repetition rate is suitable for many transonic and supersonic flow fields and imaging is possible with commercially available high-speed cameras. The total duration of this burst is 1 msec, which corresponds to the duration of the gain envelope of the power amplifier chain.

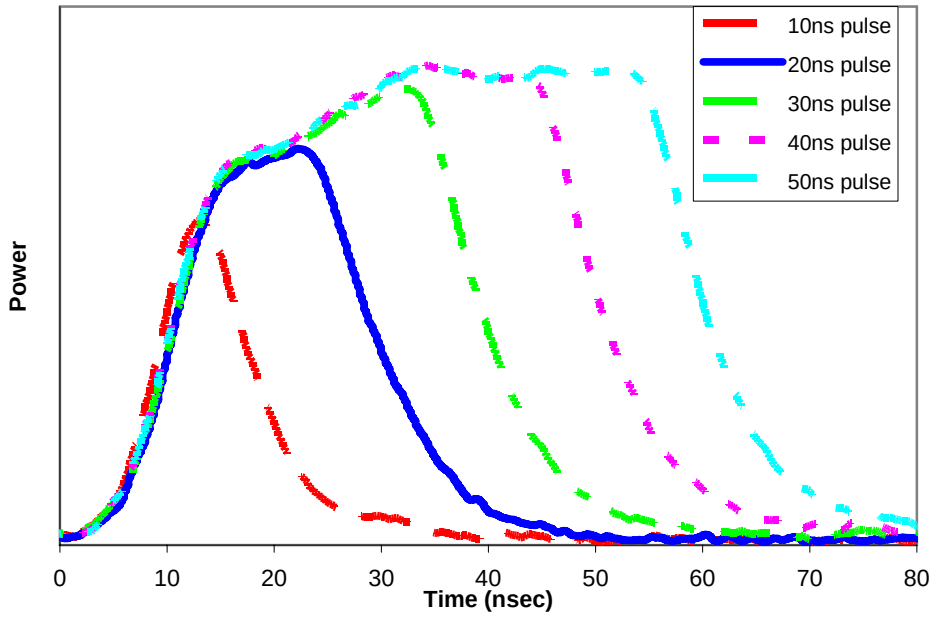

Figure 3 – Pulse shape for 10, 20, 30, 40 and 50 nsec duration pulses.

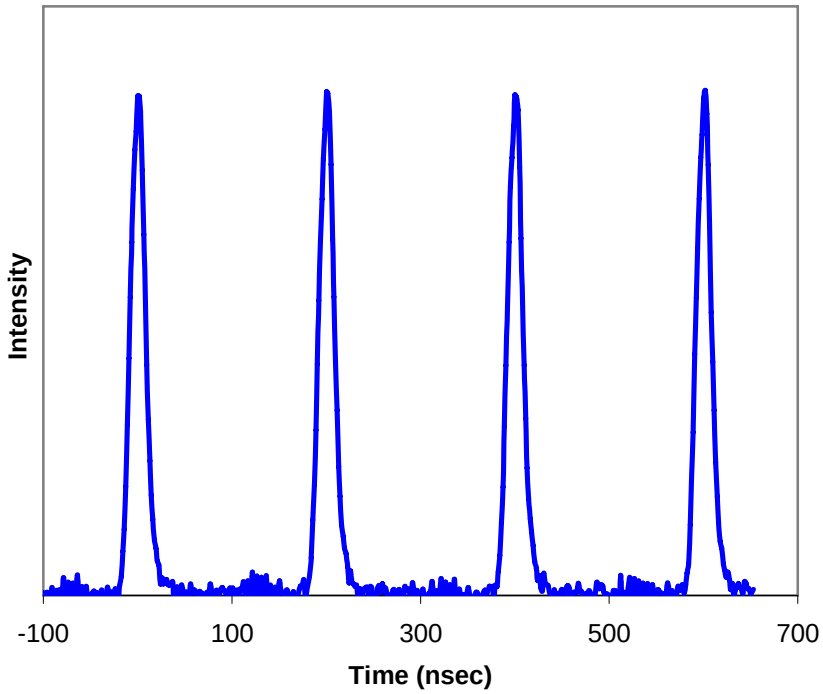

Figure 4 – A burst of four 20 nsec pulses separated by 200 nsec each (5 MHz).

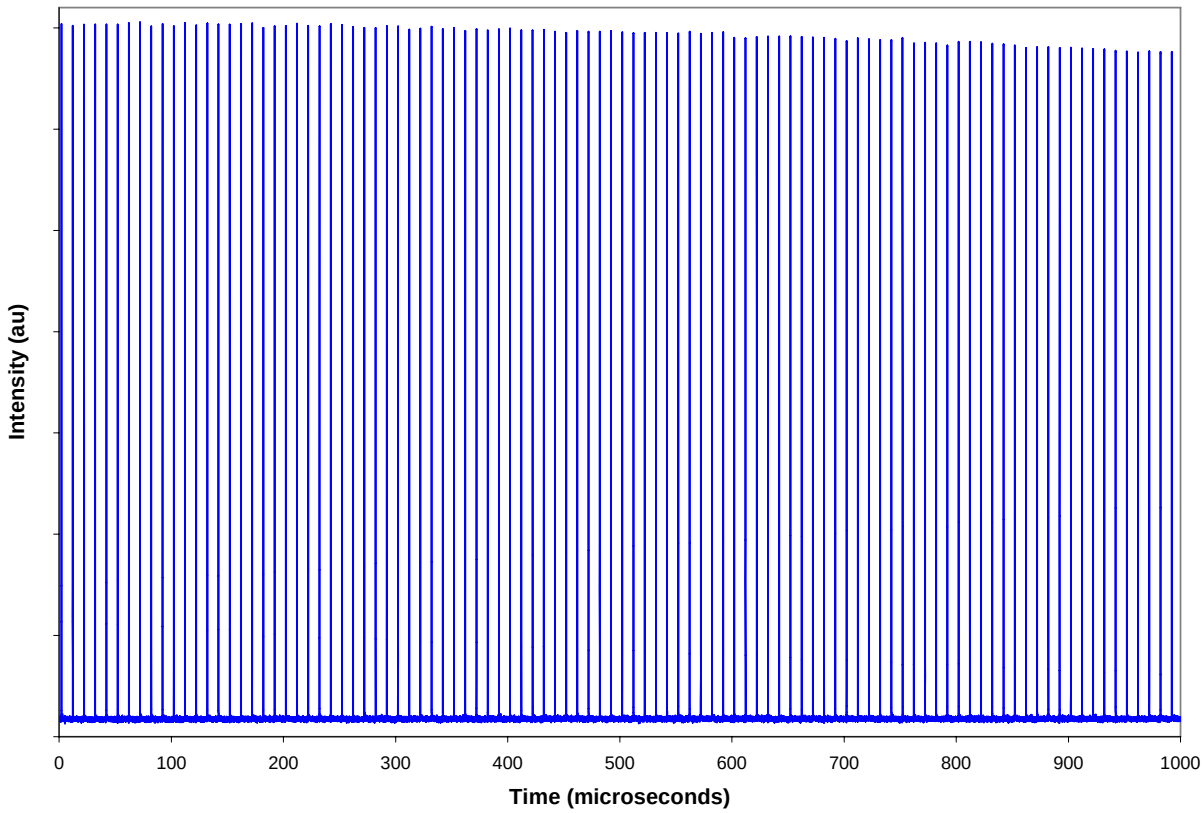

Figure 5 – Oscilloscope trace of a 100 pulse burst of pulses at 100 kHz. Each pulse is 20 nsec in duration.

One strength of the AOM pulse slicer is its flexibility. The duration of pulses and the pulse spacing is determined by a TTL voltage applied to the AOM driver. Using a computer based timing card and pulse generator, the user has maximum flexibility in determining the properties of the pulses, such as their timing and duration. In many applications, it is desired to have uniform energy contained in each pulse. The flexibility to change the pulse duration from pulse to pulse may be used to attain this goal where the pulse duration can be increased with time to offset the gain loss occurring in the system. Alternatively, many applications, particularly those associated with transient phenomena, will benefit from the ability to operate in an asynchronous fashion. With the 1 msec window of gain available, it should also be possible to synchronize the laser with random, external events.

IV. Power Amplifier Chain

Following formation of the burst of low energy pulses, the pulses must be amplified by a factor of $10^6 – 10^8$ to be useful for general fluid dynamic measurements. This amplification is provided by a chain of three flashlamp-pumped double-pass Nd:YAG rod amplifiers. Construction of the amplifier system (LaserPath Technologies, Orlando, FL) is nearly complete with final testing currently taking place. The design of the system and some preliminary measurements are reported here; a more complete characterization of the system will be the topic of a future paper.

A schematic of the power amplifier chain is shown in Figure 6 and a photo in Figure 7. The input beam (pulses) from the pulse slicer passes through a Faraday isolator and is enlarged to 4 mm in diameter with a telescope. The beam then passes through a polarizer and into the 1st amplifier, which has a diameter of 4 mm and length of 100 mm. The amplified beam (single pass) then passes through a $\lambda/4$ waveplate, reflects from a 0º mirror, travels back through the waveplate (for a net retardation of $\lambda/2$) and back through the amplifier (2nd pass) and then is reflected by the polarizer to the next amplifier. This process is repeated for the 2nd and 3rd amplifiers, which have diameters of 5 and 6.3 mm, respectively. The pulse energy supplied to the flashlamps is 20, 30 and 40 J, respectively. Optical isolators are contained between each amplification stage in an effort to minimize amplified spontaneous emission

(ASE) and parasitic lasing, problems that were significant in the early development of systems at Princeton and OSU.

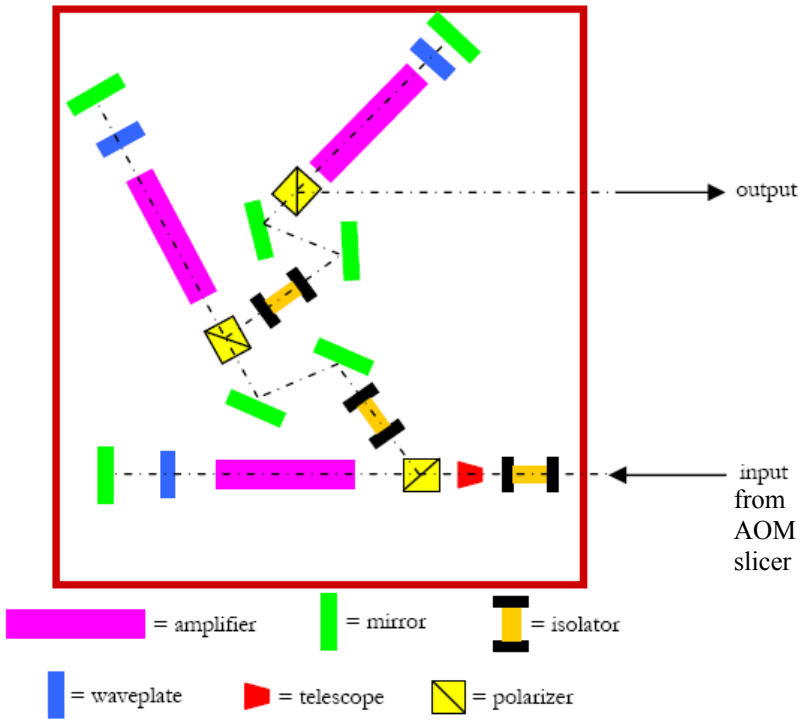

Figure 6 – Schematic of power amplifier chain for AU pulse burst laser system.

Preliminary measurements show the overall gain of the system to be greater than 10^7 for a low energy pulse input. This was confirmed at LaserPath Technology's factory where a 1.3 nJ input pulse produced by a Q-switched Nd:YAG laser was measured to have a 14 mJ output after passing through the amplifier system. This yields an overall gain for the system of ~1.1 x 10^7. This level of performance is similar to previously described systems at OSU and Princeton and can be improved through the addition of more amplifiers.

The most significant change to the AU pulse burst laser is the temporal gain curve of the amplifier chain. In previous designs, the power supply for the amplifiers was similar in design to those used in standard single-pulse Nd:YAG lasers, which did not have high repetition rate capability. As such, these systems delivered a Gaussian shaped gain curve with duration from 100-200 µsec. The energy within a pulse would thus depend on its temporal location within this period of time. For the pulse burst laser concept, this curve is superimposed on the burst of pulses making it difficult to achieve uniform energy over the entire burst of pulses. In the current design, the desired gain curve is 1 msec long with a uniform gain over that duration. This was achieved by modifying the pulse forming network that regulates current to the flashlamps. Figure 8 presents the fluorescence at 1.064 microns from one of the amplifiers, where the expected gain profile is apparent. After an initial rise time of ~250 µsec, the intensity is fairly uniform over a 1 msec timespan. The droop, or drop in signal over this time, is ~10%. Thus, we can expect to have uniform gain over this region.

A more uniform gain curve is significant as the non-uniformity of pulses has been a problem in the past, particularly when using harmonic frequencies, which have a non-linear conversion efficiency. The extension of the gain envelope to 1 msec is also quite significant in that it will allow for operation at lower repetition rates while still producing a significant number of pulses. For example, operation at a "low repetition rate" of 10 kHz would have been limited to 2-3 pulses in previous designs. In the current design, 10-11 pulses with significant energy are expected for operation at 10 kHz. This will allow the laser system to be used in a broader range of fluid dynamic applications, which may require lower repetition rates, more pulses, or both. The characteristics of the system will be examined in more detail when the system is fully complete.

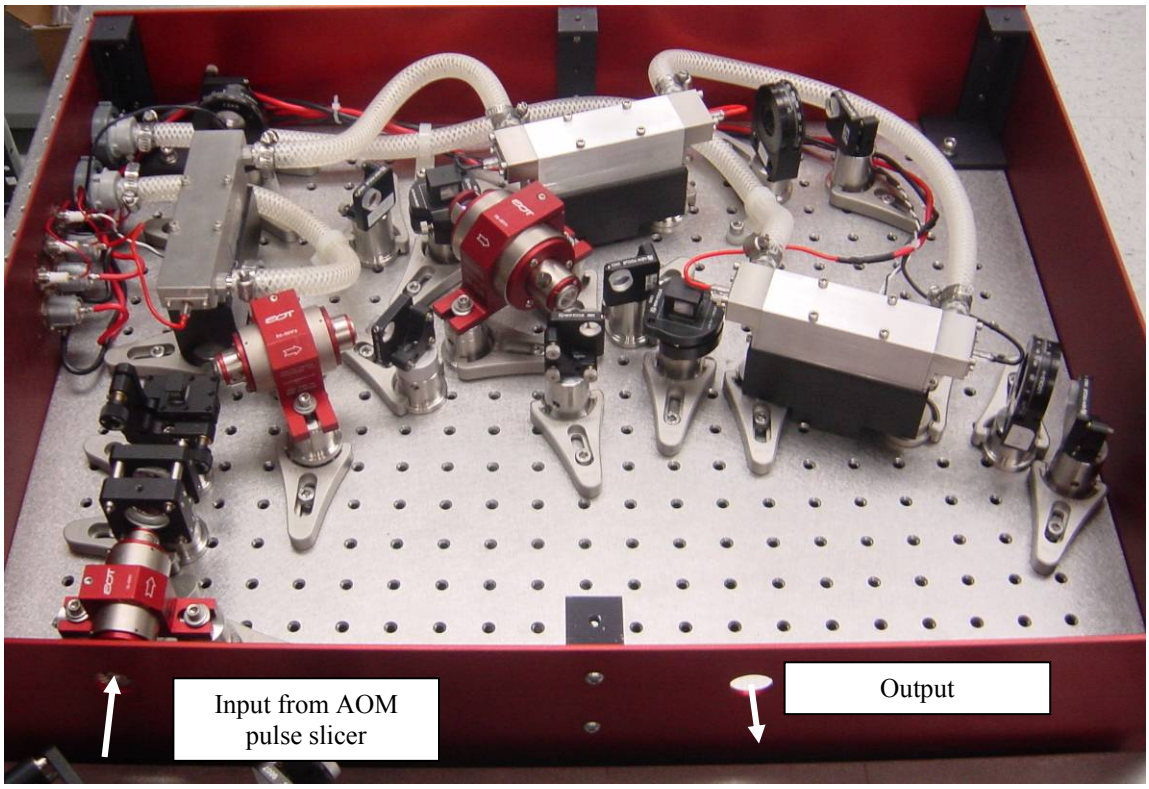

Figure 7 – Photograph of power amplifier chain for AU pulse burst laser system.

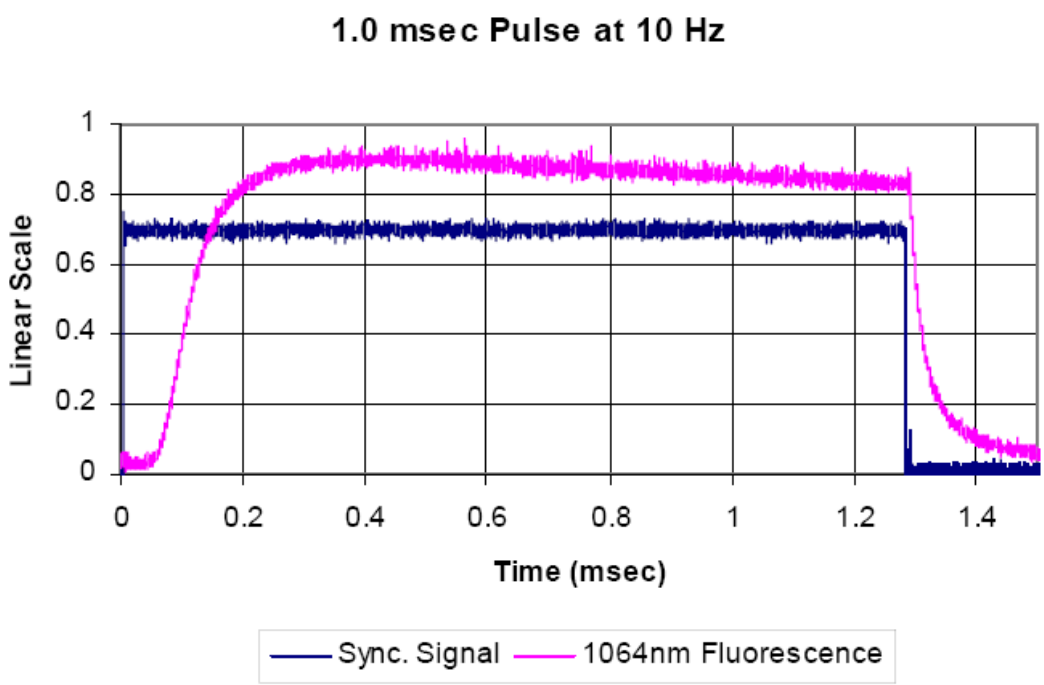

Figure 8 – Temporal gain curve of flashlamp pumped amplifiers.

V. Conclusions and Future Work

The design of a new pulse burst laser system has been presented. It is similar to previously described pulse burst laser systems except for two major changes. First, pulse slicing is achieved using an acousto-optic modulator instead of a pair of Pockels cell. The primary advantage to the AOM over Pockels cell is that the AOM is significantly cheaper (90%), while not giving up any significant capabilities. The AOM can operate at high repetition rates and with variable duration pulses. For fluid dynamic measurements, which is the ultimate goal of the authors, where short pulse durations are necessary for instantaneous measurements, pulses as short as 10 nsec have been demonstrated. In addition, these pulses are produced with a contrast ratio of ~15,000:1, which will allow the system to operate more efficiently. The second change is to the amplifier chain's power supply, which has been modified to produce uniform gain over a 1 msec timespan. This is in contrast to previous systems which had a Gaussian shaped gain curve with a 100-200 μsec timespan. Preliminary measurements with the power amplifier chain show an overall gain of $>10^7$ with a ~10% droop over the 1 msec duration of the flashlamp pulse.

Construction of the amplifier system is expected to be completed within the next few weeks. A more detailed characterization of the system will then be undertaken in which numerous effects will be explored. Of interest are the average pulse energy within a burst and the uniformity of energy between pulses. It is expected that the energy stored in the amplifiers will be depleted by each successive laser pulse faster than it can be restored when operating at high repetition rates. This will ultimately limit the amount of energy that can be put into each pulse while still maintaining a uniform distribution of energy. As mentioned, one possible method of alleviating this problem would be to make each successive pulse slightly longer in duration so that the total energy in each pulse remains constant. At lower repetition rates, however, the time between pulses should be sufficient for the depleted energy to be restored in the rods by the flashlamp pulses. This will allow the laser system to operate at "slow" repetition rates from 10 kHz to 100 kHz with pulse energies in excess of 10 mJ/pulse, characteristics that are not currently available in any other laser system.

In addition, a frequency doubling module will be added to the laser system. Most Nd:YAG lasers are capable of operating at 2nd, 3rd and 4th harmonics, with the majority of fluid dynamic applications, such as PIV and PDV, using the 2nd harmonic (532 nm) output of the laser. 2nd harmonic generation using a Type II KTP non-linear crystal has been demonstrated in other systems with 40-50% efficiency. 3rd (355 nm) and 4th (266 nm) harmonic generation are also possible with efficiencies on the order of 20-35%.

It has been demonstrated here that a pulse burst laser system using an AOM pulse slicer is an economical and feasible design. Ultimately, the purpose of this laser system is for fluid dynamic measurements. The next logical step once the laser is complete is to begin applying this unique technology towards flow measurements. Initial measurements will focus on high-repetition rate flow visualization and high-speed PIV, but plans are in place to utilize the unique capabilities of this laser system to develop new diagnostic techniques. In addition, the pulse burst laser system is modular and, therefore, easily expandable. While current pulse energies are expected to be on the order of 1-10 mJ/pulse, it is possible to increase pulse energies to the 100 mJ/pulse range through the addition of more amplifiers.

Acknowledgments

Brian Thurow would like to thank Dr. Greg Elliott (UIUC) for suggesting that an acousto-optic modulator might be capable of slicing short duration pulses from a cw laser beam. He would also like to thank Dr. Walter Lempert and Dr. Mo Samimy (OSU) for their help and guidance through graduate school and into his professional career, particularly with respect to the opportunity to work with the pulse burst laser at OSU. This work was supported using start-up funds provided by Auburn University.

References

[1] W. R. Lempert, P. Wu, B. Zhang, R. B. Miles, J. L. Lowrance, V. Mastracola, and W. F. Kosonocky, "Pulse-burst laser system for high speed flow diagnostics," AIAA Paper 96-0500 (1996).

[2] P. Wu and R.B. Miles, "High-energy pulse-burst laser system for megahertz-rate flow visualization", *Optics Letters*, Vol. 25, No. 22, pp 1639-1641, 2000.

[3] P. Wu, W. R. Lempert, and R. B. Miles, "MHz pulse-burst laser system and visualization of shock-wave/boundary-layer interaction in a Mach 2.5 wind tunnel," *AIAA J.* **38**, 672-679 (2000).

[4] B. Thurow, N. Jiang, M. Samimy, and W. Lempert, "Narrow-Linewidth Megahertz-Rate Pulse-Burst Laser for High-Speed Flow Diagnostics," Applied Optics, Vol. 43, No. 26, pp. 5064-5073 (2004).

[5] Thurow, B., Jiang, N., Lempert, W. and Samimy, M., "MHz Rate Planar Doppler Velocimetry in Supersonic Jets," AIAA Journal, Vol. 43, No. 3, pp. 500-511, March 2005.

[6] Wernet, M., and Opalski, A., "Development and application of a MHz-frame rate PIV system," AIAA Paper 2004-2184, 2004.

[7] Kastengren, A., Dutton, J. and Elliott, G., "Time-Correlated Visualizations of Supersonic Blunt-Base Cylinder Wakes," AIAA Paper 2005-1346, 43rd AIAA Aerospace Sciences Meeting and Exhibit, Reno, Nevada, Jan. 10-13, 2005

[8] B. Thurow, M. Samimy, and W. Lempert, "Compressibility Effects on Turbulence Structures in Axisymmetric Mixing Layers," Physics of Fluids, Vol. 15, No. 6, pp. 1755-1765, (2003).

[9] Hileman, J., Thurow, B., Caraballo, E. and Samimy, M., "Dynamics of Large Scale Structures and Sound Emission in High-Speed Jets: Real-time Visualization with Simultaneous Acoustic Measurements," *Journal of Fluid Mechanics,* Vol. 544, pp. 277-307, 2005.